IOP Conference Series: Materials Science and Engineering

PAPER • OPEN ACCESS

Determining of the machine compliance using instrumented indentation test and finite element method

To cite this article: D Zíta *et al* 2018 *IOP Conf. Ser.: Mater. Sci. Eng.* **461** 012095

Determining of the machine compliance using instrumented indentation test and finite element method

D Zíta[1], P Hanus[1,2], E Schmidová[1] and J Zajíc[1]

[1]University of Pardubice, Studentská 95, 53210 Pardubice, Czech Republic

[2]petr.hanus@upce.cz

Abstract. At present time the importance of indentation measurements once again increases. As modern and perspective measurement method it allows to measure various mechanical properties while only needing micro volumes of materials. While standard hardness measurement methods examine only the plastic response of sampled material, Depth Sensing Indentation (DSI) testing is founded on real-time recording of applied force and resulting travel of indenter. This allows to evaluate both plastic and elastic response of examined material during the indentation process which in turn allows for calculation of various static material properties in very small volumes of samples. The big advantage of this approach is saving of time (especially on sample preparation), however the data analysis – and thus results – could be influenced by certain factors. Those worth noting are surface quality of the sample, wear of the indenter head, its shape and material, and also the compliance of testing machine's frame. If we consider the frame of testing machine having non-zero compliance, inevitably there will occur not only displacement of indenter but also displacement of frame itself, especially noticeable while using high loads. This negatively influences the results of such measurement. This work's aim is to calculate the compliance of test machine's frame using Finite Element Method model and 1 mm in diameter steel ball indenter. The result of this work is addition of virtual spring to the FEM model and fine tuning of its stiffness. This should allow us to minimize the influence of frame's compliance on the results of future measurements.

1 Introduction

Indentation tests are one of the most common techniques for the local mechanical characterization of materials. Different numerical models have been developed to predict uniaxial mechanical properties using different indenter geometries – mainly spherical, cone, pyramidal and flat-ended cylinder. Elastic-plastic models are established to simulate the response of load-displacement curve during the loading-unloading process, detail discussions reflect connected problems [1, 2, 3]. The indentation of an elastic-plastic material is a problem difficult to be solved analytically, because of the unknown shape and extension of the plastic field [4, 5].

Different effects are the part of current research in the contact mechanics nowadays, to provide precise estimation of local mechanical parameters by indentation test. Effect of edge compliance on the contact mechanics of rigid spherical indenters in adhesive contact has been already investigated as a function of applied load [6]. Due to the considered adhesive interaction, qualitative and quantitative changes were observed in the stress and deformation fields. The effect of the edge compliance was also detailed in measurable quantities like indentation depth and contact stiffness. An inverse procedure, starting from experimentally measured pairs of load and depth of penetration, followed by an extensive finite element modelling of the indentation process gave an accurate reproduction of elastic–plastic properties [7, 8]. Some current results indicate the significant decrease of indentation resistance compared to real tensile tests [9]. The same problem, i.e. calibration issues in real indenter geometry and frame compliance in spherical nanoindentation was investigated using two different methodologies; fitting the Hertz equation to force–depth data for indentation and profiling the residual impression for indentation depths, which led to a large discrepancy in effective radii [10]. Research of composites is mainly focused on the influence of the tip defect on the determination of the mechanical properties using Berkovich, Vickers, Knoop and spherical indenters [11].

Finite element analysis presents the approach which requires suitable experimental validation. Considering the tests particular conditions, indentation process needs to be defined according the testing conditions. Relatively close agreement between experiment and simulation can be achieved considering the strain incremental extension. Comparatively less success is attained in matching numerical and experimental results presumably because of the effects of anisotropy. Stain rate dependence and/or heterogeneities at the microstructural level not captured by the constitutive theory used in the simulations. The sensitivity of numerical results to indenter imperfection and indenter elasticity has been subjected to current research. The effect of friction and specimen creep during indentation on load-displacement predictions is also assessed [12].

Surface quality conditions, temperature as well as a local material heterogeneity can influence the accuracy of obtained material parameters. Presented work was devoted to problem of loading system compliance, methodology of numerical assessment was suggested, and final experimental validation was performed.

The basic foundations for this article are measurements curves obtained from fully-instrumented universal hardness measurement machine Zwick ZHU/Z2.5Z. These measurements were conducted using 1 mm in diameter spherical indenter pushed into bainite steel, using maximum force of 300 N. The output of the measurement is force-depth loading curve. This dependency is however influenced by compliance of the frame of the test machine. To acquire the compliance of the frame we use Finite Elements Methods model and using this we calculate expected real behavior of used samples. In next step the FEM model is adjusted by addition of spring element simulating the compliance of the machine's frame. The final goal is to fine tune parameters of this added spring to obtain as similar as possible values in real-life measurement and in FEM model.

2 Model

All of the performed FEM calculations were done using commercially available solver ABAQUS 6.17. Two different samples were simulated, the first one representing linear-elastic material, the second one being elastic-plastic material based on real tensile test results of bainite steel. The first one is used to validate the model by comparing the results of numerical calculation and analytic solution based on Hertz theory. Both models use ideally rigid spherical indenter with 1 mm diameter and axisymmetric cylindric sample with height of 4.4 mm and radius also 4.4 mm.

Boundary conditions are very similar to all models. Zero displacement in the direction perpendicular to the axis of symmetry is used for nodes on this axis (AB), zero displacement in direction perpendicular to baseline is prescribed for nodes on this baseline (BD) – figure 1. Loading is applied by forced displacement of the indenter. For model with added spring representing compliance of frame of test machine nodes on the baseline are connected to one node of spring using stiff kinematic coupling. The other node has zero displacement and zero rotations in all directions. This represents spring with one degree of freedom – displacement in direction of the indenter displacement.

Between the surface of indenter and upper surface of sample the contact "surface to surface" is prescribed. With elastic sample the coefficient of friction is f=0, in other cases it is f=0.1.

The mesh of the sample is made up of three- and four-nodes 2D axisymmetric elements (CAX). Smallest dimension of elements (in area of contact between sample and indenter) is 3 μm. The total number of elements is 28 800.

IOP Conf. Series: Materials Science and Engineering **461** (2019) 012095 doi:10.1088/1757-899X/461/1/012095

The results of this simulation are shown on figure 2 – Von Mises stress with maximum load and after loading.

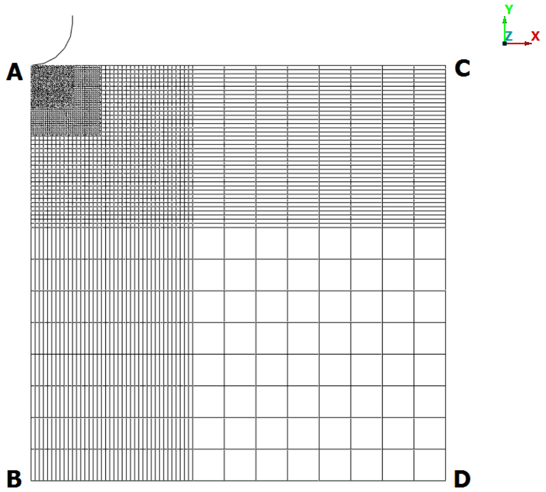

Figure 1. FEM mesh

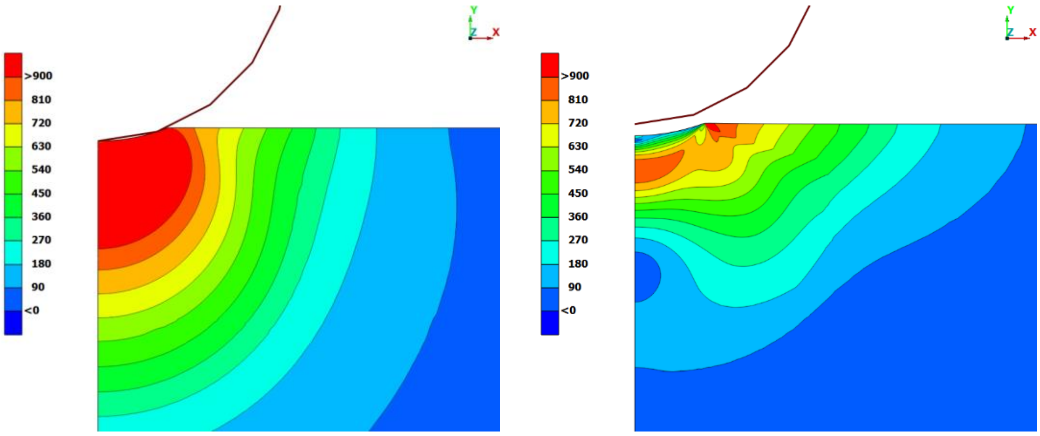

Figure 2. Von Mises stress with maximum load (left) and after loading (right)

2.1 Linear elastic sample

To validate the model the results of numerical calculations were compared with analytical solution of equations (1), (2) and (3) based on Hertz theory [13]. Material of the sample is in this case linear-elastic with Young's modulus $E = 210$ MPa.

$$\sigma_x = -p_{max} \cdot \left[\left(1 - \left| \frac{z}{a} \right| \cdot \tan^{-1} \left| \frac{a}{z} \right| \right) \cdot (1 + \nu) - \frac{1}{2 \cdot \left(1 + \frac{z^2}{a^2} \right)} \right] \quad (1)$$

$$\sigma_z = \frac{-p_{max}}{1 + \frac{z^2}{a^2}} \quad (2)$$

$$\sigma_{Tresca} = \sigma_x - \sigma_z \quad (3)$$

where z is depth below surface, a is radius of contact area, p_{max} is maximum pressure on the center of contact surface and σ_{Tresca} is the equivalent Tresca's stress. On figure 3 the good match between numerical and analytical solutions for depth of indentation 10 µm is clearly visible.

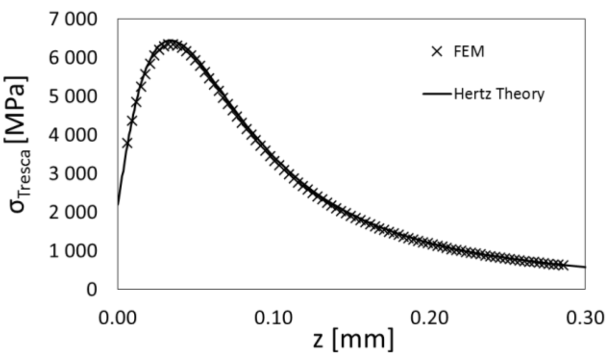

Figure 3. Comparison of analytical and FEM solution

2.2 Bainite steel, elastic–plastic sample

Elastic-plastic sample has linear behavior up to yield strength with Young's modulus $E = 210$ GPa. After this point the stress-strain dependency is taken directly from results of tensile strength test – as can be seen on figure 4. Stiffness characteristic of the spring representing compliance of the frame is presented on figure 5.

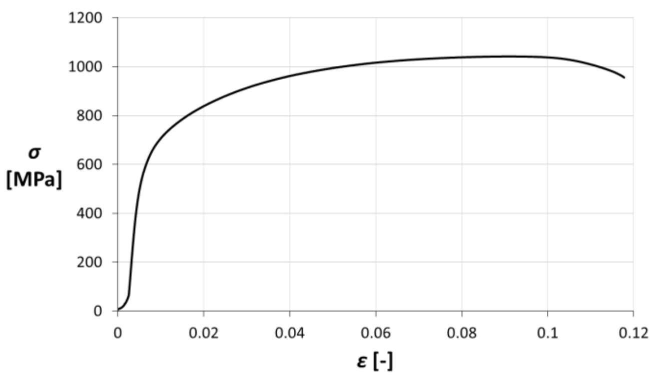

Figure 4. Tensile test curve (True Stress - Strain)

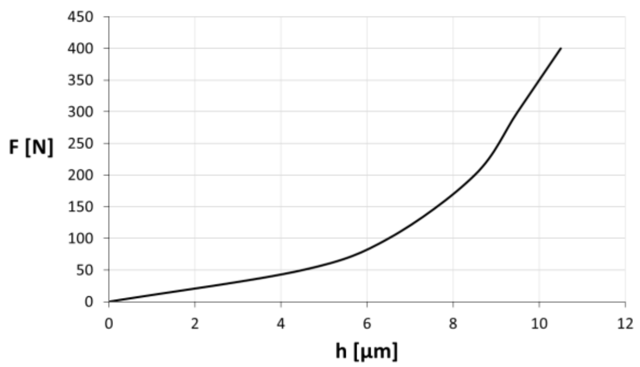

Figure 5. Characteristic of the spring

3 Results

Figure 6 shows comparison between FEM analyses with completely rigid frame and with added spring representing real frame's compliance and also with real test record. It can be clearly seen that there is a significant difference between real test and model using completely rigid frame. On the other hand, the model with added spring (representing frame's compliance C_f – figure 7) shows very good match with real test. This is caused by deformation happening not only to sample but also to test machine's frame and to the indenter.

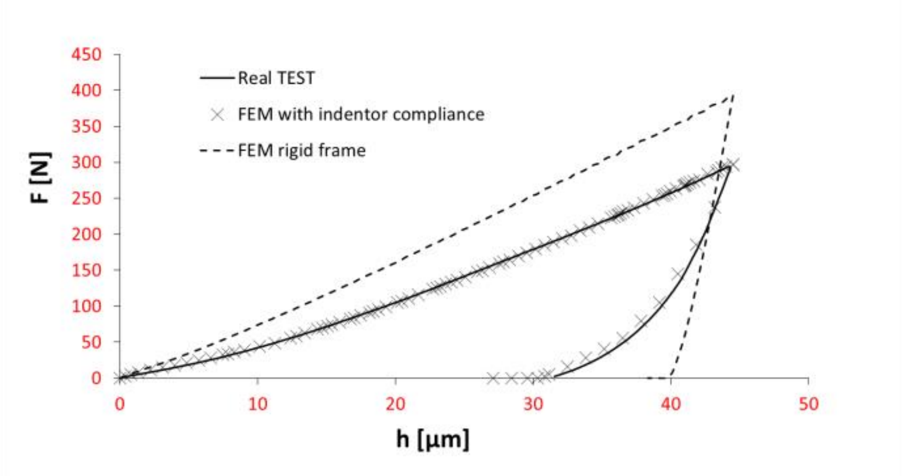

Figure 6. Indentation curves

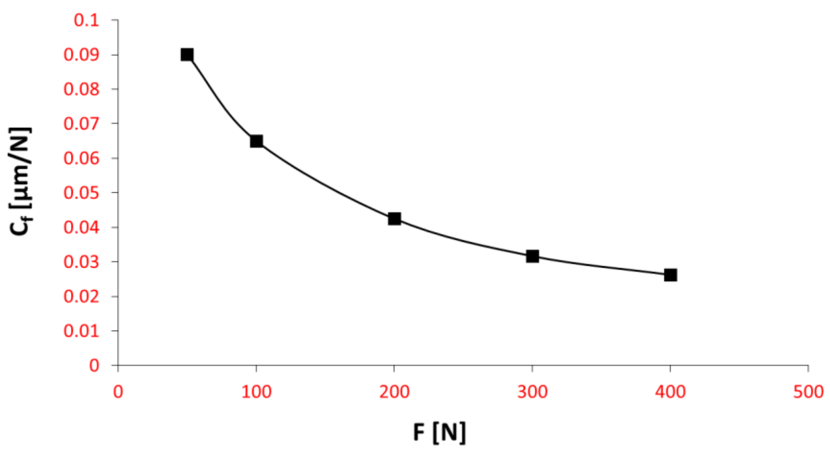

Figure 7. Indenter frame compliance C_f

The curve on figure 6 was constructed using iteration methods – by minimizing of difference between measured indentation curve and indentation curve obtained from FEM analysis with added spring. Effects of surface roughness and indenter wear are both included in compliance of frame. We expect negligible effect of surface roughness as the samples were finely grinded (roughness approximately Ra = 0.8). For the purpose of FEM simulation, we used ideal shape of indenter.

4 Summary

It is necessary to mention that the computed compliance of the frame also contains compliance of the indenter and also the effect of surface roughness and free travel of parts of test machine. The next planned step is to evaluate the compliance with real-life experiment which will show the impact of said parameters.

Acknowledgements
Made with support of project no. FV30149 “3D printing of numerically optimized steel parts using DMLS technology”.

References
[1] Chen R et al. 2015 Numerical simulation of spherical indentation method to identify metal material mroperties *Adv. Mat. Res.* 1119 pp 779-82
[2] Lee H, Lee J H and Pharr G M 2005 A numerical approach to spherical indentation techniques for material property evaluation *J Mech. and Phys. of Sol.* 53 p 2037-69
[3] Kang J J, Becker A A, Wen W and Sun W 2018 Extracting elastic-plastic properties from experimental loading-unloading indentation curves using different optimization techniques *Int. J. Mech. Sc.* 144 pp 102-9
[4] Riccardi B and Montanari R 2004 Indentation of metals by a flat-ended cylindrical punch *Mat. Sc. and Eng.* A 381 pp 281-91
[5] Puchnin M, Anisimov E, Cejp J, Kunka I and Vicens S 2014 Advantages of express-methods in investigation of mechanical and physical properties of aluminum alloys *Man. Tech.* 14 pp 234-38.
[6] Stan G 2018 The effect of edge compliance on the adhesive contact between a spherical indenter and a quarter space *Int. J. Sol. and Struct.* pp 1-11
[7] Beghini M, Bertini L and Fontanari V 2006 Evaluation of the stress–strain curve of metallic materials by spherical indentation *Int. J. Sol. and Struct.* 43 pp 2441-59
[8] Pham T H, Phan Q M and Kim S E 2018 Identification of the plastic properties of structural steel using sherical indentation *Mat. Sc. and Eng.* A 711 pp 44-61
[9] Wu J, Wang M, Hui Y, Zhang Z and Fan H 2018 Identification of anisotropic plasticity properties of materials using spherical indentation imprint mapping *Mat. Sc. and Eng.* A 723 pp 269-78
[10] Kang S, Kim Y, Lee Y, Kim J and Kwon D 2012 Determining effective radius and frame compliance in spherical nanoindentation *Mat. Sc. and Eng.* A 538 pp 58-62
[11] Chicot D, de Baets P, Staia M H, Puchi-Cabrera E S, Louis G, Perez Delgado Y and Vleugels J 2013 Influence of tip defect and indenter shape on the mechanical properties determination by indentation of a TiB2–60%B4C ceramic composite *Int. J. of Ref. Met. and H. Mat.* 38 pp 102-10
[12] Syngellakis S et al. 2018 Finite element simulation of spherical indentation experiments *Int. J. Comp. Meth. and Exp. Meas.* 6 (4) pp 749-63
[13] Johnson K L 1985 Contact mechanics, (Cambridge University Press, Cambridge)